

Cite this: *RSC Adv.*, 2017, 7, 33162Received 28th April 2017
Accepted 26th June 2017

DOI: 10.1039/c7ra04793b

rsc.li/rsc-advances

A phase-reversible Pd containing sphere-to-bridge-shaped peptide nanostructure for cross-coupling reactions†

Seongsoo Kim,^{‡a} Hong-Jun Cho,^{‡b} Namhun Lee,^a Yoon-Sik Lee,^{*b}
Dong-Sik Shin^{‡c} and Sang-Myung Lee^{*a}

A sphere-to-bridge-shaped peptide nanostructure was constructed from a tyrosine-rich peptide (H-YACAYY-OH) *via* mediating Pd²⁺ ions as well as changing temperature. This novel assembly technique provided a recyclable Pd nano-catalyst with a function of reversible thermal phase transition between the homogeneous and heterogeneous states for cross-coupling reactions.

Natural peptides coordinated with various metal ions *via* amide bonds and functional groups on side chains can form various self-assembled structures.¹ For example, ferritin is a natural intracellular protein which takes a specific conformation through interactions between peptide building blocks and Fe²⁺ ions. Artificial peptides that provide natural or non-natural metal binding sites have been developed to construct metal ion-induced self-assemblies of nanostructures including tubular-, fibre-, vesicle-, spherical-, and rod-coil-type ones.² Such metal coordination can initiate intermolecular self-assembly by bringing two or more peptides into close proximity.³ Furthermore, several metal ions coordinated with peptides have been involved in a redox reaction to induce irreversible peptide cross-linking *via* covalent bonding *e.g.*, dityrosine formation.^{4–7}

Based on a peptide template, various types of metal-peptide nanostructures have been designed and utilized as electrochemical sensors,⁸ biological scaffolds,^{9,10} and catalysts.^{11–13} In particular, significant effort has been devoted in developing metal nanoparticles (NPs)-incorporated peptide nanostructures which can then be used as catalysts in C–C coupling reaction. To facilitate the reaction, for instant, Knecht group synthesized various shapes of Pd nanostructures with a large surface area by using a self-assembling peptide template composed of R5 peptide.¹⁴ Moreover, peptide amphiphiles possessing both

hydrophobic carbon-chain and ionic peptide sequences are promising as bio-inspired-templates for growing PdNPs-incorporated nanofibers. Recently, several groups have demonstrated nanofiber incorporated with PdNPs using a self-assembled peptide amphiphile. The peptide-templated PdNPs showed high catalytic activity for the Suzuki coupling reaction under environmentally-friendly conditions.^{15,16} Although these peptide-templated PdNPs can afford efficient catalytic activities for the C–C coupling reactions, drawbacks originated from the heterogeneous state limits its broad and practical application of the catalyst.

A recent report has revealed that a tyrosine-rich peptide, YYACAYY (YC₇), can be self-assembled into a two-dimensional peptide nanostructure *via* interaction of tyrosines and cysteines leading to cross-linking at an air/water interface.¹⁷ Based on this finding, we have successfully designed Pd²⁺-ion-mediated sphere-to-bridge-shaped peptide nanostructures (YC₇@Pd²⁺) through thermally induced phase transition. During the transition, the Pd²⁺ ions have interacted with the YC₇ peptide molecules through coordination, which might be a crucial driving force for leading to a distinctive self-assembled sphere-to-bridge peptide nanostructure. More interestingly, the self-assembled YC₇@Pd²⁺ is dissolved into the aqueous solution *via* thermal transition during cross-coupling process over phase transition temperature and followed by re-assembly under the critical temperature achieving the PdNP-captured astrocyte-shaped peptide nanostructures (YC₇@PdNP). This provides a great opportunity to take advantage of YC₇@Pd²⁺ as a versatile and recyclable catalyst, capitalizing both of its homogeneous characteristic over critical temperature and heterogeneous characteristic under the same temperature. Herein, we demonstrate the feasibility of YC₇@Pd²⁺ as a new type of catalyst under environmentally friendly conditions: (a) as a nano-catalyst during C–C coupling reactions; and (b) as a heterogeneous catalyst for separation, especially in Suzuki and

^aDepartment of Chemical Engineering, Kangwon National University, Gangwon-do 24341, Republic of Korea. E-mail: sangmyung@kangwon.ac.kr; Fax: +82 33 251 3658; Tel: +82 33 250 6335

^bSchool of Chemical and Biological Engineering, Seoul National University, Seoul 08826, Republic of Korea. E-mail: yslee@snu.ac.kr; Fax: +82 2 880 1604; Tel: +82 2 880 7073

^cDepartment of Chemical and Biological Engineering, Sookmyung Women's University, Seoul 04310, Republic of Korea. E-mail: dshin@sm.ac.kr; Fax: +82 2 2077 7450; Tel: +82 2 2077 7236

† Electronic supplementary information (ESI) available. See DOI: 10.1039/c7ra04793b

‡ The authors contributed equally to this work.



Sonogashira coupling reactions. $\text{YC}_7@Pd^{2+}$, this catalytic system *via* switchable phase enabled reusable catalyst. To the best of our knowledge, this kind of the reassembly process is first demonstrated in this paper.

YC_7 is a random coil-dominant peptide, which self-assembles in an aqueous phase into a two-dimensional nanostructure.¹⁷ From this peptide, we synthesized sphere-to-bridge-type peptide nanostructures ($\text{YC}_7@Pd^{2+}$) *via* thermally controlled and Pd^{2+} -ion-mediated ionic interactions (Scheme 1). During heating the peptide up to 90 °C for 1 h, it was allowed to completely dissolve in water. As the peptide solution was gradually cooled to 60 °C, YC_7 underwent a rapid transition into a secondary, α -helix-dominant structure. At this stage, Pd^{2+} ions were injected to induce distinctive Pd-peptide secondary structures *via* ionic interactions between phenolate anions of tyrosyl residues (or C terminal carboxylate anions) and Pd^{2+} ions. Without Pd^{2+} ions, YC_7 molecules were self-assembled into irregular shaped nanostructures and nano-sheets during the thermodynamic transition (90 °C \rightarrow 60 °C) *via* interactions between tyrosines and cysteine crosslinking (Fig. S1†). However, the $\text{YC}_7@Pd^{2+}$, which was self-assembled by interactions with Pd^{2+} ions, was uniform and spherical with an average diameter of 88 ± 31 nm (count: 100) and further formed linked networks of sphere-to-bridge shapes (Fig. 1a and b). Physicochemical characterization of the nanostructure was performed with several analytical methods. First, the constituent elements of $\text{YC}_7@Pd^{2+}$, including Pd, N, O, S and Cl, were analysed by energy-dispersive X-ray microanalysis mapping (Fig. S2†). The results demonstrated that $\text{YC}_7@Pd^{2+}$ was composed of Pd^{2+} ions, evenly distributed within the YC_7 matrix.

To analyse the structure of $\text{YC}_7@Pd^{2+}$ and the interactions between Pd^{2+} ions and the peptides, it was further characterized by infrared (IR) spectroscopy (Fig. 2). Bands from $\nu(\text{C-O})$, $\nu(\text{CC})$, $\delta(\text{COH})$ of Tyr in YC_7 peptide were observed at 1070–1270 cm^{-1} ,

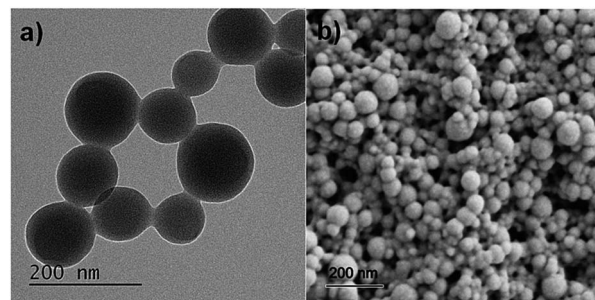
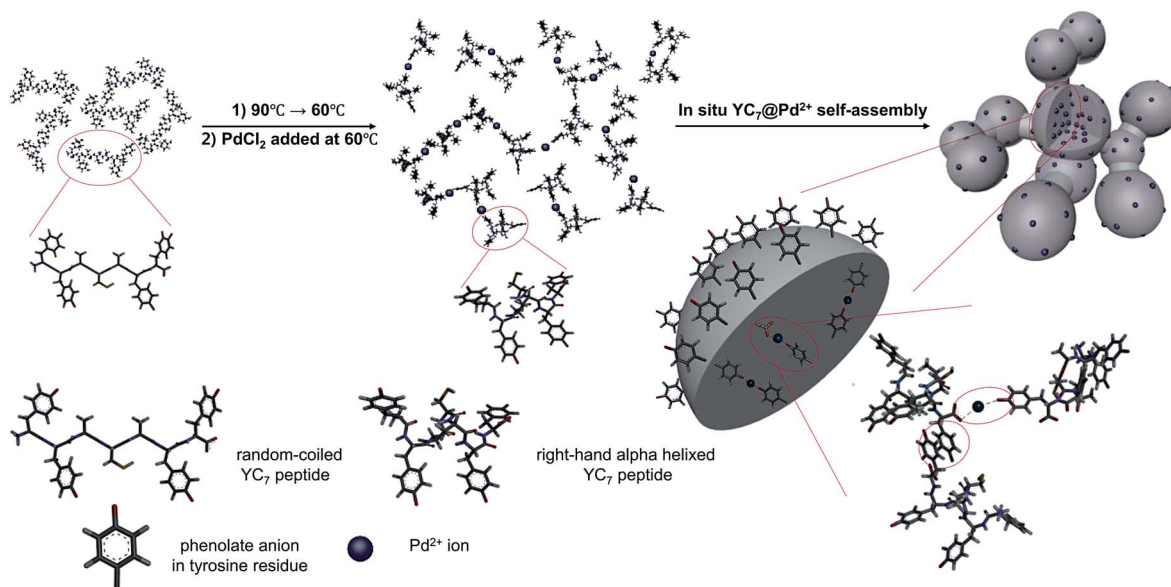


Fig. 1 (a) TEM image and (b) SEM image of $\text{YC}_7@Pd^{2+}$ nanostructure.

which exhibited relatively strong intensity due to its polar character (Fig. 2). These peaks are unique in Tyr not in other residues of YC_7 peptide. When the C–O stretching vibration bands of the self-assembled YC_7 and $\text{YC}_7@Pd^{2+}$ were compared, $\text{YC}_7@Pd^{2+}$ gave strong peaks at 1232 cm^{-1} involving two stretching modes of $\nu(\text{C}=\text{C})$ and $\nu(\text{C-O})$ in Tyr–OH, which are attributed to stronger polarity of phenolate (Tyr residue) in the presence of Pd^{2+} .^{18–21} These results clearly show that there are strong interactions between Pd^{2+} ions and tyrosine groups of $\text{YC}_7@Pd^{2+}$. In addition, a new C=O stretching vibration from the carboxylate of $\text{YC}_7@Pd^{2+}$ appeared at 1557 cm^{-1} which corresponds to the asymmetric stretching vibration of metal carboxylates.²²

Additionally, the X-ray photoelectron spectroscopy (XPS) data of $\text{YC}_7@Pd^{2+}$ clearly revealed Pd peaks ($3d_{5/2}$ and $3d_{3/2}$) at 343.20 and 337.95 eV which corresponded to Pd(II) (Fig. S3†).²³ Taken together, $\text{YC}_7@Pd^{2+}$ is a non-crystalline peptide complex coordinated with Pd(II) at tyrosine residues, and has a potential as a Pd catalyst used in C–C coupling reactions. Consequently, Pd^{2+} -ion-mediated peptide self-assembly was well characterized with IR and XPS.

Hence, this proves that the phenolate and carboxylate groups of $\text{YC}_7@Pd^{2+}$ were primarily involved in coordination with Pd^{2+}



Scheme 1 Proposed mechanism of $\text{YC}_7@Pd^{2+}$ synthesis by thermal phase transition of dissolved YC_7 and Pd^{2+} -ion-driven self-assembly.



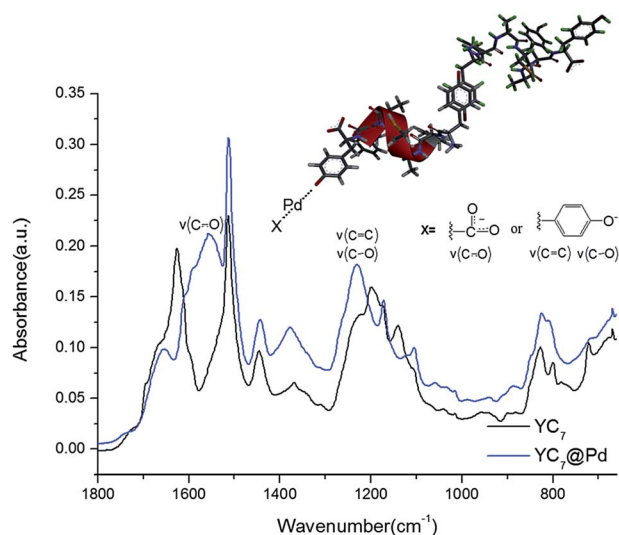


Fig. 2 FT-IR spectra of $\text{YC}_7\text{@Pd}^{2+}$ and YC_7 peptide.

ions leading to the formation of a distinctive Pd-peptide nanostructure. Inductively coupled plasma atomic emission spectroscopy (ICP-OES) analysis revealed that the palladium content of $\text{YC}_7\text{@Pd}^{2+}$ was calculated to be 1.86 mmol Pd per g catalyst.

The X-ray diffraction (XRD) patterns of self-assembled YC_7 exhibited distinctive peaks at 10° and 18° originating from the intersheet reflections of peptide sheets, respectively (Fig. S4†). In contrast, peptide sheet-originated regular sharp peaks of face-centered cubic Pd crystals did not appear in the XRD pattern of $\text{YC}_7\text{@Pd}^{2+}$ (Fig. S5†). This result supports that Pd^{2+} ions were able to collapse the intrinsic YC_7 structure, leading to the irregular shaped peptide arrangement inside the sphere-to-bridge-shaped peptide nanostructure.

We investigated the catalytic activity of the $\text{YC}_7\text{@Pd}^{2+}$ by evaluating the efficiency of C–C coupling reactions including Suzuki, Heck and Sonogashira coupling reactions.²⁴ Actually, $\text{YC}_7\text{@Pd}^{2+}$ nanostructures are decomposed into the solution at coupling reaction temperature, and then PdNPs instantly reduced from Pd^{2+} ions participate in the three kinds of coupling reactions. First, various bases for each coupling reaction were screened in aqueous solution.²⁵ K_2CO_3 and pyrrolidine were selected as the best base in the Suzuki and the Sonogashira reactions, respectively. (Tables S1 and S2†). However, the catalytic activity of $\text{YC}_7\text{@Pd}^{2+}$ in the Heck coupling reactions gave unfavourable yields (<2%) even in the presence of cetyl trimethyl ammonium bromide (CTAB) (Table S3†).²⁶ Therefore, $\text{YC}_7\text{@Pd}^{2+}$ was further used as a catalyst for the Suzuki and the Sonogashira coupling reactions of aryl iodides with phenylboronic acid or phenylacetylene in an aqueous solvent system at 80°C , where $\text{YC}_7\text{@Pd}^{2+}$ can be transformed into the homogeneous phase.

An activated aryl iodide (4-iodoacetophenone) was well-converted to the corresponding biaryl compounds in the Suzuki coupling reaction with over 98% yield in only 1 h with 0.1 mol% of $\text{YC}_7\text{@Pd}^{2+}$ (Table 1, entry 1). Electron-donating substituents lowered the yields of the corresponding biaryl

Table 1 Suzuki–Miyaura coupling reactions for various aryl iodides in the presence of $\text{YC}_7\text{@Pd}^{2+}$ catalyst^a

$\text{R}-\text{C}_6\text{H}_4-\text{I} + \text{C}_6\text{H}_5-\text{B}(\text{OH})_2 \xrightarrow[\text{K}_2\text{CO}_3, \text{H}_2\text{O}, 80^\circ\text{C}]{\text{YC}_7\text{@Pd}^{2+}} \text{R}-\text{C}_6\text{H}_4-\text{C}_6\text{H}_5$ <p>or 2-iodothiophene</p>			
Entry	R	Time (h)	Yield ^c (%)
1	COCH_3	1	98.7
2	OH	3	99.6
3	OCH_3	3	92.8
4	H	3/3 ^b	88.8/99.9 ^b
5	CH_3	6/3 ^b	70.8/96.0 ^b
6	2-Iodothiophene	6/3 ^b	40.0/91.3 ^b

^a Conditions: aryl iodine and heterocyclic halides (0.155 mmol), phenylboronic acid (0.186 mmol), $\text{YC}_7\text{@Pd}^{2+}$ (0.1 mol%), K_2CO_3 (0.274 mmol) in water (1 mL) at 80°C . ^b GC yields when 0.5 eq. of CTAB was used. ^c GC yields.

compounds (Table 1, entries 2–5). In particular, the oxygen-containing substrates (Table 1, entries 2 (OH) and 3 (OMe)) exhibited more efficient coupling than non-oxygen-containing substrates. These results demonstrated that the hydrogen bonding facilitated the access of $\text{YC}_7\text{@Pd}^{2+}$ to the substrate molecules under aqueous conditions providing a compatible coupling environment for the Suzuki coupling reaction. Furthermore, the use of CTAB as a phase-transfer catalyst promoted the interphase transfer of substrates, thereby boosting the coupling yields of the non-oxygen containing substrates (Table 1, entries 4 (H) and 5 (Me)). As a control experiment, compared with the coupling reaction catalyzed by $\text{YC}_7\text{@Pd}^{2+}$, the coupling yields by PdCl_2 activation were lower than those of $\text{YC}_7\text{@Pd}^{2+}$ in same condition (Table S4†).

Given the successful catalytic activity of $\text{YC}_7\text{@Pd}^{2+}$ in the Suzuki coupling reactions, we further investigated the catalytic activity of $\text{YC}_7\text{@Pd}^{2+}$ in the Sonogashira coupling reactions with CuI under aqueous conditions.²⁷ The Sonogashira coupling reaction catalysed by $\text{YC}_7\text{@Pd}^{2+}$ exhibited a high coupling yield with a strong electron-withdrawing substrate (Table S5,† entry 1). In contrast to the Suzuki coupling reaction, the hydrogen bonding derived from the electron-donating substrates (Table S5,† entries 3 and 6) was not relatively effective on the catalytic activity in the Sonogashira coupling reaction. CTAB strongly suppressed the cross-coupling reaction, and instead, accelerated homo-coupling reaction with activated aryl iodide. The results indicate that CTAB did not afford a compatible cross-coupling environment between the catalyst and the substrates in the Sonogashira coupling reaction, whereas it stabilized phenylacetylene with Cu^+ ion to activate the homo-coupling pathway.

During the coupling reaction at 80°C in an aqueous solvent, $\text{YC}_7\text{@Pd}^{2+}$ disassembled into a soluble Pd-peptide complex, which is reduced into the solubilized PdNP catalyst. After cooling down to room temperature, the PdNP-peptide complex was reassembled and transformed into a nanostructure which is similar with a shape of astrocyte ($\text{YC}_7\text{@PdNP}$, Fig. S6b†). This reversible process between homogeneous and heterogeneous



states facilitated easy isolation and reuse of $\text{YC}_7\text{@PdNP}$ from the reaction mixture. To evaluate the reusability of $\text{YC}_7\text{@Pd}^{2+}$, the catalyst was recycled in subsequent Suzuki coupling reactions with 4-iodophenol or 4-iodoacetophenone. While the coupling yields of the activated substrates (iodoacetophenone) decreased slightly in the fourth and fifth runs, 4-iodophenol which can form a hydrogen bonding with $\text{YC}_7\text{@PdNP}$ was converted to the corresponding biaryl compound in excellent yields (yield > 98%) even after 5th use (Fig. S7†).⁹ These results reconfirm that hydrogen bonding enabled the substrates for easy access to the Pd-peptide complex as well as possibly stabilizing the PdNPs for excellent catalytic activity during a series of Suzuki coupling reactions.

In conclusion, we developed a novel method for the construction of Pd^{2+} -ion-mediated sphere-to-bridge-shaped peptide nanostructures, $\text{YC}_7\text{@Pd}^{2+}$, of which morphology can be controlled by temperature in an aqueous phase. Characterized by the switchable thermally-reversible phase transition, $\text{YC}_7\text{@Pd}^{2+}$ acted as a solubilized nano-catalyst during C–C coupling reactions and reassembled into a heterogeneous structure for isolation and reuse after each coupling reaction. $\text{YC}_7\text{@Pd}^{2+}$ showed an excellent activity as a catalyst for the Suzuki and the Sonogashira coupling reactions under aqueous conditions. Especially, in the Suzuki coupling reaction, hydrogen bonding capability of the substrates provided a favourable coupling environment, enhancing the coupling yield and reusability of the catalyst. The morphology controllable self-assembled Pd^{2+} -ion-mediated peptide nanostructure can open a new avenue as a reusable catalyst for C–C coupling reactions under environmentally-friendly conditions.

Acknowledgements

This work was supported by the Ministry of Science, ICT & Future Planning and National Research Foundation of Korea through Basic Science Research Program (NRF-2014R1A1A1006711), the Ministry of Trade, Industry & Energy (MOTIE), Korea Institute for Advancement of Technology (KIAT) through the Encouragement Program for The Industries of Economic Cooperation Region (R0004027) and Kangwon National University through 2015 Research Grant (No. 520150081).

Notes and references

- O. Yamauchi, A. Odani and M. Takani, *J. Chem. Soc., Dalton Trans.*, 2002, 3411–3421.
- R. Zou, Q. Wang, J. Wu, J. Wu, C. Schmuck and H. Tian, *Chem. Soc. Rev.*, 2015, **44**, 5200–5219.
- M. M. Pires, D. E. Przybyła, C. M. R. Perez and J. Chmielewski, *J. Am. Chem. Soc.*, 2011, **133**, 14469–14471.
- T. G. Huggins, M. C. W. Knecht, N. A. Detorie, J. W. Baynes and S. R. Thorpe, *J. Biol. Chem.*, 1993, **268**, 12341–12347.
- S. Takasaki, Y. Kato, M. Murata, S. Homma and S. Kawakishi, *Biosci., Biotechnol., Biochem.*, 2005, **69**, 1686–1692.
- Y. K. A. Hilaly, T. L. Williams, M. S. Parker, L. Ford, E. Skaria, M. Cole, W. G. Bucher, K. L. Morris, A. A. Sada, J. R. Thorpe and L. C. Serpel, *Acta Neuropathol. Commun.*, 2013, **1**, 1–17.
- K.-I. Min, G. Yun, Y. Jang, K.-R. Jim, Y. H. Ko, H.-S. Jang, Y.-S. Lee, K. Kim and D.-P. Kim, *Angew. Chem., Int. Ed.*, 2016, **55**, 6925–6928.
- S. Kim, J. H. Kim, J. S. Lee and C. B. Park, *Small*, 2015, **11**, 3623–3640.
- T. Mizutaru, T. Sakuraba, T. Nakayama, G. Marzun, P. Wagener, C. Rehbock, S. Barcikowski, K. Murakami, J. Fujita, N. Ishiie and J. Yamamoto, *J. Mater. Chem. A*, 2015, **3**, 17612–17619.
- Y.-X. Pan, H.-P. Cong, Y.-L. Men, S. Xin, Z.-Q. Sun, C.-J. Liu and S.-H. Yu, *ACS Nano*, 2015, **9**, 11258–11265.
- D. B. Pacardo, M. Sethi, S. E. Jones, R. R. Naik and M. R. Knecht, *ACS Nano*, 2009, **3**, 1288–1296.
- W. Wang, C. F. Anderson, Z. Wang, W. Wu, H. Cui and C.-J. Liu, *Chem. Sci.*, 2017, **8**, 3310–3324.
- W. Wang, Z. Wang, M. Yang, C.-J. Zhong and C.-J. Liu, *Nano Energy*, 2016, **25**, 26–33.
- A. Jakhmola, R. Bhandari, D. B. Pacardo and M. R. Knecht, *J. Mater. Chem.*, 2010, **20**, 1522–1531.
- I. Maity, D. B. Rasale and A. K. Das, *RSC Adv.*, 2014, **4**, 2984–2988.
- M. A. Khalily, O. Ustahuseyin, R. Garifullin, R. Genc and M. O. Guler, *Chem. Commun.*, 2012, **48**, 11358–11360.
- H.-S. Jang, J.-H. Lee, Y.-S. Park, Y.-O. Kim, J. Park, T.-Y. Yang and Y.-S. Lee, *Nat. Commun.*, 2014, **5**, 3665–3675.
- M. S. Shongwe, C. H. Kaschula, M. S. Adsetts, E. W. Ainscough, A. M. Brodie and M. J. Morris, *Inorg. Chem.*, 2005, **44**, 3070–3079.
- A. Barth, *Prog. Biophys. Mol. Biol.*, 2000, **74**, 141–173.
- L. I. Grace, R. Cohen, T. M. Dunn, D. M. Lubman and M. S. D. Vries, *J. Mol. Spectrosc.*, 2002, **215**, 204–219.
- L. Rodriguez, E. Labisbal, A. S. Pedrares, J. A. G. Vazquez, J. Romero, M. L. Duran, J. A. Real and A. Sousa, *Inorg. Chem.*, 2006, **45**, 7903–7914.
- V. Otero, D. Sanches, C. Montagner, M. Vilarigues, L. Carlyle, J. A. Lopes and M. J. Melo, *J. Raman Spectrosc.*, 2014, **45**, 1197–1206.
- G. Kumar, J. R. Blackburn, R. G. Albridge, W. E. Moddeman and M. M. Jones, *Inorg. Chem.*, 1972, **11**, 296–300.
- T. Suzuka, K. Kimura and T. Nagamine, *Polymers*, 2011, **3**, 621–639.
- I. Hoffmann, B. Blumenroder, S. O. N. Thumann, S. Dommer and J. Schatz, *Green Chem.*, 2015, **17**, 3844–3857.
- P. Qiu, J. Y. Zhao, X. Shi and X. H. Duan, *New J. Chem.*, 2016, **40**, 6568–6572.
- A. M. Thomas, A. Sujatha and G. Anilkumar, *RSC Adv.*, 2014, **4**, 21688–21698.

